Research Article

The PKA Signaling Pathway Regulates the Association of the Autophagy Initiation Complex With the Lipidation Machinery

Miranda Bueno-Arribas [1], Celia Cruz-Cuevas [1], Beatriz Monforte-Martinez [1], María-Angeles Navas [2], Ricardo Escalante [1], andOlivier Vincent [1,*]

*1 - **Instituto de Investigaciones Biomédicas Sols-Morreale CSIC-UAM,** 28029 Madrid, Spain*
*2 - **Departamento de Bioquímica y Biología Molecular,** Facultad de Medicina, Universidad Complutense de Madrid, Madrid, Spain*

***Correspondence to Olivier Vincent:** o.vincent@csic.es (O. Vincent)*
https://doi.org/10.1016/j.jmb.2025.168954
Editor: Martens Sascha

Abstract

A key step in autophagy is the conjugation by the E3-like Atg12-Atg5-Atg16 complex of the ubiquitin-like protein Atg8 to phosphatidylethanolamine on the autophagosomal membrane, a process known as lipidation. Previous work in yeast showed that recruitment of the E3-like complex to the preautophagosomal structure is mediated by the interaction of Atg16 with the phosphatidylinositol 3-phosphate-binding protein Atg21, and by the association of Atg12 with the scaffold protein of the Atg1 kinase complex, Atg17. Here, we conducted a reverse two-hybrid screen to identify residues in Atg17 and Atg12 critical for Atg17-Atg12 binding, and used these data to generate a docking model of Atg12-Atg5-Atg16 with the Atg17 complex. In this model, a conserved alpha-helix in the N-terminal region of Atg12 binds to the convex side of crescent-shaped Atg17 and appears to form a four-helix bundle with the three helices of Atg17, similar to that described for the binding of Atg31 to Atg17. We further showed that, in agreement with previous work, Atg17-Atg12 and Atg21-Atg16 binding act cooperatively to mediate the recruitment of the E3-like complex, although our results show that alternative mechanisms are involved in this process. Finally, we found that phosphorylation of Atg12 by PKA prevents its interaction with Atg17, thus adding a new regulatory layer in the control of autophagy by the PKA signaling pathway.

Introduction

Autophagy is a process of degradation and recycling of cytosolic components such as proteins or organelles, which is activated in response to nutrient starvation and is essential to maintain cellular homeostasis. This process occurs through the formation of a double membrane structure, the phagophore, which expands to sequester the cargo to be degraded, giving rise to a vesicle called the autophagosome. The autophagosome then fuses with the lysosome/vacuole, leading to the degradation of its contents.

This process requires the sequential assembly of different protein complexes formed by Atg proteins at the preautophagosomal structure (PAS), which is adjacent to both the endoplasmic reticulum (ER) and vacuole.[1] The autophagic machinery is highly conserved in eukaryotes and was initially characterized in the model yeast *Saccharomyces cerevisiae*. In yeast, the autophagy initiation complex also called the Atg1 kinase complex includes the Atg17-Atg29-Atg31 subcomplex, which homod-

imerizes and serves as a platform for the recruitment of Atg13, which binds the Atg1 kinase.[2,3] The presence of two Atg17 binding sites in Atg13 leads to the multimeric assembly of Atg1 complexes, a key step for the autophosphorylation and activation of this kinase and the recruitment of Atg9-containing vesicles, which likely act as a seed membrane for phagophore formation.[4–6] Activated Atg1 phosphorylates multiple components of the autophagic machinery and enables recruitment of phosphatidyl-inositol-3-kinase complex 1 and formation of phosphatidyl-inositol-3-phosphate (PtdIns3P) at the phagophore membrane.[7,8] PtdIns3P triggers the recruitment of PtdIns3P-binding proteins of the PROPPIN/WIPI family, Atg18 and Atg21.[9] Atg18 forms a complex with Atg2, a protein that transfers lipids from the ER to the phagophore to promote its elongation,[10–13] while the interaction of Atg21 with Atg16 mediates the recruitment of the E3-like Atg12-Atg5-Atg16 complex that conjugates the ubiquitin-like protein Atg8 to phosphatidylethanolamine on the autophagosomal membrane, in a process termed lipidation.[6,14–16] Atg12 is another ubiquitin-like protein that conjugates with Atg5 and associates with Atg16 to form the E3-like complex.[17,18]

A previous study suggested that the recruitment of the Atg12-Atg5-Atg16 complex to the PAS depends not only on the interaction of Atg16 with the PtdIns3P-binding protein Atg21, but also involves the interaction of Atg12 with the scaffold protein Atg17 of the autophagy initiation complex.[19] Here, we have carried out a mutagenic analysis to identify the binding residues in Atg12 and Atg17 and, based on these data, to model the complex formed by Atg12-Atg5-Atg16 and the Atg17 subcomplex. Furthermore, we have functionally characterized the corresponding mutants and confirmed that this interaction cooperates with that mediated by Atg16 and Atg21 in the recruitment of the E3-like complex, although our results suggest that additional mechanisms mediate this key step in autophagy. Finally, we have shown that phosphorylation of Atg12 by PKA prevents its binding to Atg17, revealing an additional layer of autophagy regulation by this kinase.

Results

Identification of the Atg12 binding site in Atg17

A previous study suggested that binding of Atg12 to Atg17 mediates the association between the Atg12-Atg5-Atg16 E3-like complex and the Atg1 kinase complex, and that the N-terminal region of Atg12 is involved in this interaction.[19] To ensure that this association only involves Atg12 and not the other subunits of the E3-like complex, we analyzed the interaction of Atg17 with Atg5, Atg16, Atg12 and the Atg12 N-terminal region (residues 1–100) using the two-hybrid system. We found that Atg17 interacts solely with Atg12, specifically with the N-terminal region of this protein (Figure 1A). Additionally, we confirmed that although they do not interact with Atg17, both Atg5 and Atg16 bind to Atg16 (Figure 1A).

In order to determine which residues in Atg17 are critical for binding Atg12, we performed a reverse double two-hybrid screen (RD2H).[20] This method allows the identification of missense mutations that specifically prevent protein–protein interactions. We first generated random mutations in a two-hybrid fusion protein containing Atg17 fused to a C-terminal PTAP motif. Then, we used a dual reporter system to select Atg17 mutants that have lost the ability to interact with Atg12 without preventing PTAP binding to the TSG101 human protein. This selection eliminates all C-terminal truncating mutations that remove the PTAP motif, or mutations that destabilize the fusion protein. We repeatedly identified three missense mutations in Atg17 that disrupt Atg12 binding without preventing PTAP-mediated interaction with TSG101 (first two panels in Figure 1B). One of the mutated residues (M91V/M91T) is located in helix α1, whereas the other two (L137S and L141P) are located in helix α2 (Figure 1C, top). Notably, the three mutated residues are in close proximity in the 3D structure of Atg17, supporting the idea that they form the Atg12 binding site (Figure 1C, below). Moreover, this region of Atg17 is distinct from those involved in the interaction with other proteins of the Atg17 complex such as Atg13, the Atg29-Atg31 complex, or Atg17 itself via dimerization (Figure 1C). However, given the proximity between the corresponding binding sites, we wanted to ensure that these mutations specifically disrupt Atg12 binding without affecting the formation of the Atg17 complex. Two-hybrid assays show that none of these mutations prevent Atg13 and Atg31 binding, or Atg17 dimerization (Figure 1B). To confirm these results, we analyzed the effect of these mutations on Atg17-Atg12 binding in Glutathione S-transferase (GST) pulldown assays. First, we showed that purified, bacterially expressed GST-Atg12 binds to Flag-Atg17 from yeast cell extracts, supporting the idea that this interaction is direct (Figure 1D). In addition, and in agreement with the two-hybrid data, we found that all three mutations prevent *in vitro* binding of Atg17 to Atg12 (Figure 1D). Western blot analysis further showed that these mutations do not affect substantially the stability of Atg17 (Figure 1D).

A previous study demonstrated that the recruitment of the Atg12-Atg5-Atg16 E3-like complex to the PAS involves two mechanisms: one mediated by the interaction of Atg12 with Atg17, and another mediated by the interaction of Atg16 with the PtdIns3P-binding protein, Atg21.[19] Accordingly, blocking one of these mechanisms only results in a partial defect in autophagy.[19] Based on this model, inactivating the Atg12 binding site in Atg17 should also lead to a partial reduction in autophagic flux. To test this hypothesis, we

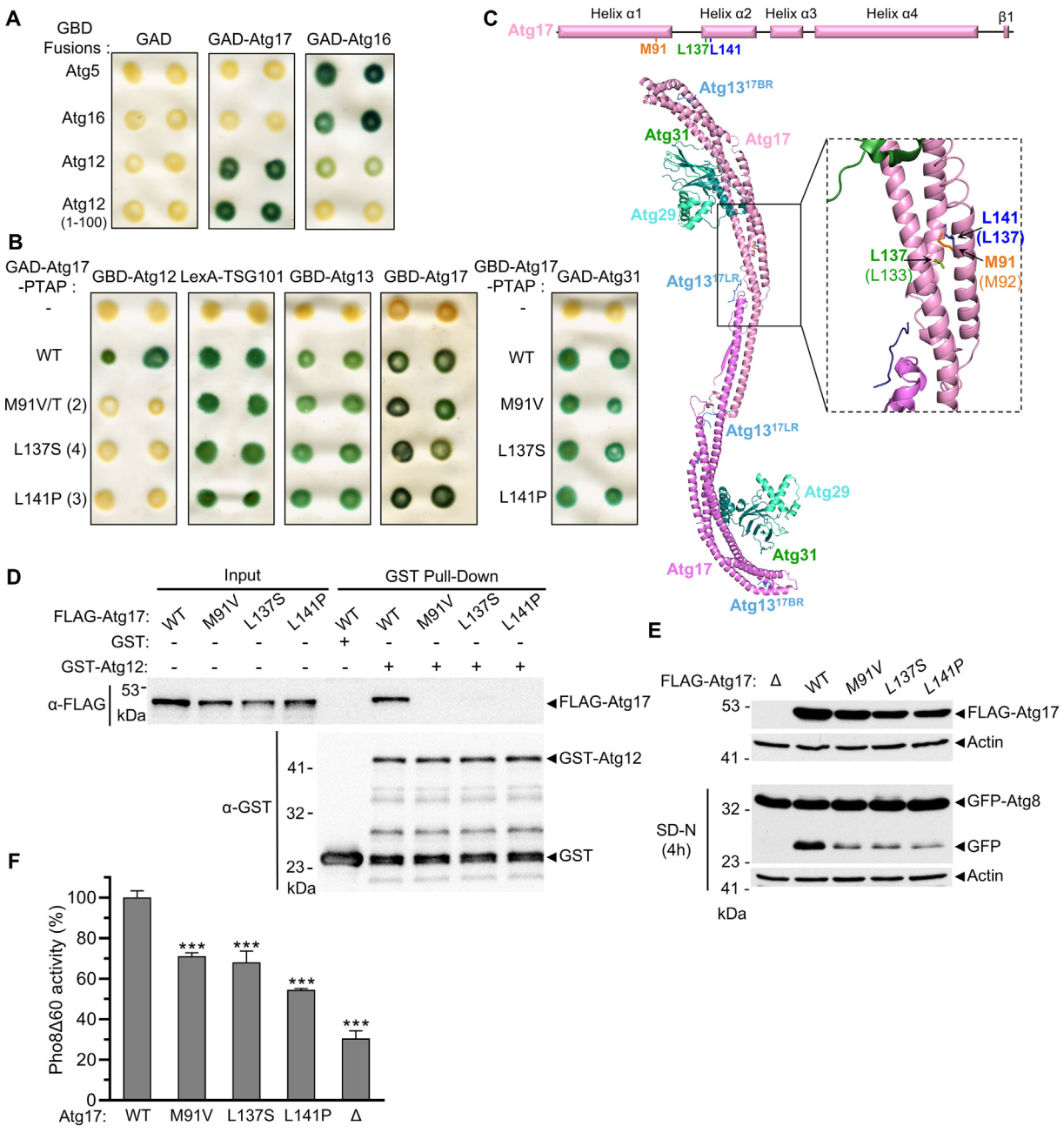

Figure 1. Characterization of the Atg12 binding site in Atg17. (**A, B**) GBD, GAD and LexA fusions proteins and the indicated mutant derivatives were tested for two-hybrid interaction in X-gal filter assays. Numbers in parenthesis in B indicate the number of times the indicated amino acid substitutions were identified in the screen. (**C**) (Top) Position of the mutated residues in Atg17. (Bottom) PyMOL structure of the Atg13^{17LR}-Atg13^{17BR}-Atg17-Atg29-Atg31 complex from *Lachancea thermotolerans* containing the Atg17-Atg29-Atg31 dimer and the Atg13^{17LR} and Atg13^{17BR} peptides (PDB: 5JHF). (Right) Enlarged view showing the mutated residues in *S. cerevisiae* as colored sticks. The corresponding residues in *L. thermotolerans* are shown in parenthesis. (**D**) Pull-down assay of Flag-Atg17 and the indicated mutant derivatives with GST-Atg12 or GST. Input represents 1.5% of protein extract used for binding experiment. (**E**) OVY404 was cotransformed with pGFP-Atg8 and either p3FLAG-Atg17 (WT), the indicated mutant derivatives or vector control (Δ). Cells were starved 4 h in SD-N medium and protein extracts were immunoblotted with anti-GFP or anti-actin antibodies. Protein extracts from mid-log phase cells were immunobloted with anti-FLAG or anti-actin antibodies. (**F**) OVY415 was transformed with p3FLAG-Atg17 (WT), the indicated mutant derivatives or vector control (Δ). Cells were starved 4 h in SD-N medium and the ALP activity was measured and normalized to WT (100%). The mean values are shown with standard deviation (n = 3); Asterisks above error bars indicate significant differences with WT. ***p > 0.001 (One-way Anova).

expressed near-endogenous levels of the Atg17 mutant proteins in a *atg17Δ atg11Δ* strain and analyzed the processing of green fluorescent protein-Atg8 fusion (GFP-Atg8) to free GFP to monitor the progression of autophagy after a shift to nitrogen-free medium (SD-N)[21] (Figure 1E). The *atg11Δ* background was used to prevent GFP-Atg8 processing mediated by the Cytoplasm-to-vacuole targeting (Cvt) pathway. We found that GFP-Atg8 processing is partially defective in all three mutants, demonstrating that inactivation of the Atg12 binding site in Atg17 partially compromises autophagy (Figure 1E). To further quantify the effect of these mutations on autophagic flux, we performed an alkaline phosphatase (ALP) assay using a truncated form of the Pho8 phosphatase (Pho8Δ60), which requires autophagy for transport and activation in the vacuole.[21] We found that all three mutations cause a partial blockage of autophagy, confirming the results obtained with GFP-Atg8 (Figure 1F).

Identification of the Atg17 binding site in Atg12

Reciprocally, we performed a reverse two-hybrid screen to identify the residues in Atg12 that mediate the interaction with Atg17. We generated random mutations in an Atg12-PTAP fusion and identified four missense mutations (R53G, L54S, S55P, and L57P) that disrupt Atg17 binding without preventing the PTAP-mediated interaction with TSG101 (Figure 2A). Following the same procedure as previously mentioned, we showed that these mutations prevent GST-Atg12 binding to Flag-Atg17 in pulldown assays and do not seem to alter the stability of the protein (Figure 2B). It is noteworthy that the four mutated residues are in close proximity and located in the N-terminal region of Atg12 (Figure 2C), in agreement with the two-hybrid mapping analysis (Figure 1A). In addition, these four residues are part of a conserved motif in Atg12 orthologs within the *Saccharomyces* clade (Figure 2C).

Following the same approach as for Atg17, we examined whether the inactivation of the Atg17 binding site in Atg12 also results in a partial defect in autophagic activity. We found that GFP-Atg8 processing to free GFP after a shift to nitrogen-free medium (SD-N) is indeed partially decreased (Figure 2D). This reduction in the mutants is also detected in the ALP assay, with a decrease in ALP activity (Figure 2E).

In a previous study, it was shown that the N-terminal truncation of 56 amino acids in Atg12 (ΔN56), which removes the Atg17 binding site we have identified, also results in a partial reduction of autophagy.[19] We found that the effect on autophagy of this truncating mutant and one of the missense mutants (R53G) is similar, demonstrating that the mutations identified in the reverse two-hybrid screen also result in a complete inactivation of the Atg17 binding site (Figure 2F, left). Western blot analysis further showed that these mutations do not alter the levels of the Atg5-Atg12 conjugate (Figure 2F, right).

Molecular modeling of the Atg17-Atg12 interaction

We used the HADDOCK server to dock the Atg12-Atg5-Atg16 and Atg17 complexes, and the residues identified by reverse two-hybrid analysis were introduced as ambiguous interaction constraints to drive the docking process. According to the docking model, Atg12 binds to the convex side of the crescent structure of each Atg17 monomer, in a region located between the Atg31 binding site and the dimerization domain (Figure 3, middle). In this model, the critical residues of Atg12 identified in our study are located at the end of an α-helix (Figure 3, left), which corresponds to the conserved motif identified in the N-terminal region of Atg12 (Figure 2C). Strikingly, this helix appears to form a four-helix bundle with the three helices of Atg17,

Figure 2. Characterization of the Atg17 binding site in Atg12. (**A**) GAD, GBD and LexA fusions proteins and the indicated mutant derivatives were tested for two-hybrid interaction in X-gal filter assays. (**B**) Pull-down assay of Flag-Atg17 with GST-Atg12, the indicated mutant derivatives or GST. Input represents 1.5% of protein extract used for binding experiment. (**C**) Sequence alignment of the N-terminal region of Atg12 (aa 1–100) in the indicated yeast species, using T-Coffee and Boxshade servers. Identical residues are shaded in black and similar residues in grey. Arrowheads indicate the position of the mutated residues, and brackets indicate a PKA phosphorylation consensus sequence. (**D**) OVY467 was cotransformed with pGFP-Atg8 and either p3HA-Atg12 (WT), the indicated mutant derivatives or vector control (Δ). Cells were starved 4 h in SD-N medium and protein extracts were immunoblotted with anti-GFP or anti-actin antibodies. Protein extracts from mid-log phase cells were immunobloted with anti-HA or anti-actin antibodies. (**E, F**) OVY463 was transformed with p3HA-Atg12 (WT), the indicated mutant derivatives, or vector control (Δ). Cells were starved 4 h in SD-N medium and the ALP activity was measured and normalized to WT (100%). The mean values are shown with standard deviation ($n = 3$); Asterisks above error bars indicate significant differences WT. *$p > 0.05$, **$p > 0.01$, ***$p > 0.001$, ns: non-significant (One-way Anova). (**F**, Right) Protein extracts from the indicated transformants grown to mid-log phase were immunoblotted with anti-HA antibody to detect free HA-Atg12 and HA-Atg12-Atg5 conjugates. A non-specific band is indicated by an asterisk.

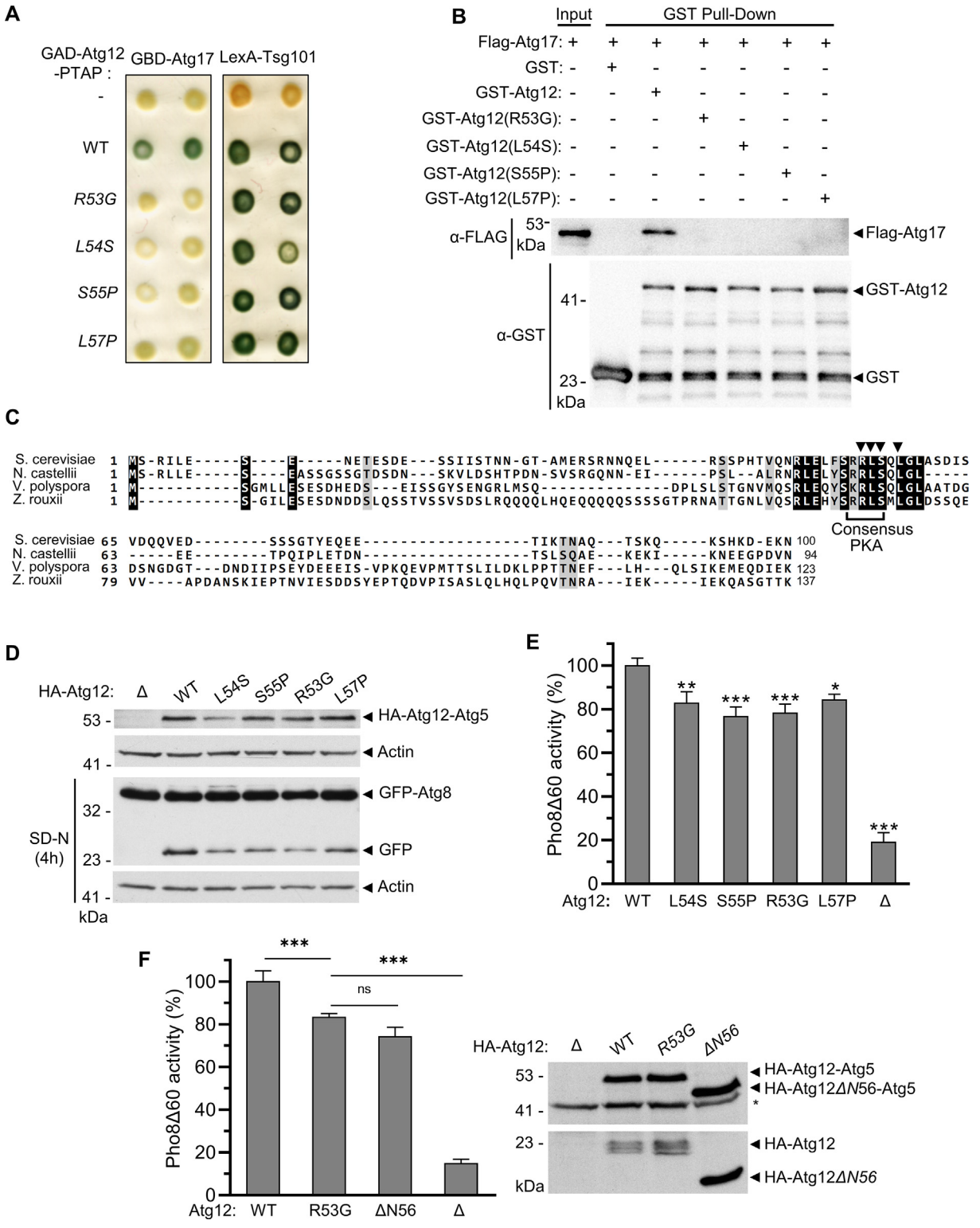
A
GAD-Atg12 -PTAP :
GBD-Atg17
LexA-Tsg101
-
WT
R53G
L54S
S55P
L57P
B
Input
GST Pull-Down
Flag-Atg17:
GST:
GST-Atg12:
GST-Atg12(R53G):
GST-Atg12(L54S):
GST-Atg12(S55P):
GST-Atg12(L57P):
α-FLAG
53-
kDa
Flag-Atg17
α-GST
41-
23-
GST-Atg12
GST
C
S. cerevisiae
N. castellii
V. polyspora
Z. rouxii
Consensus PKA
D
HA-Atg12:
Δ
WT
L54S
S55P
R53G
L57P
HA-Atg12-Atg5
Actin
GFP-Atg8
GFP
SD-N (4h)
kDa
E
Pho8Δ60 activity (%)
Atg12:
WT
L54S
S55P
R53G
L57P
Δ
F
ns
Atg12:
WT
R53G
ΔN56
Δ
HA-Atg12-Atg5
HA-Atg12ΔN56-Atg5
HA-Atg12
HA-Atg12ΔN56

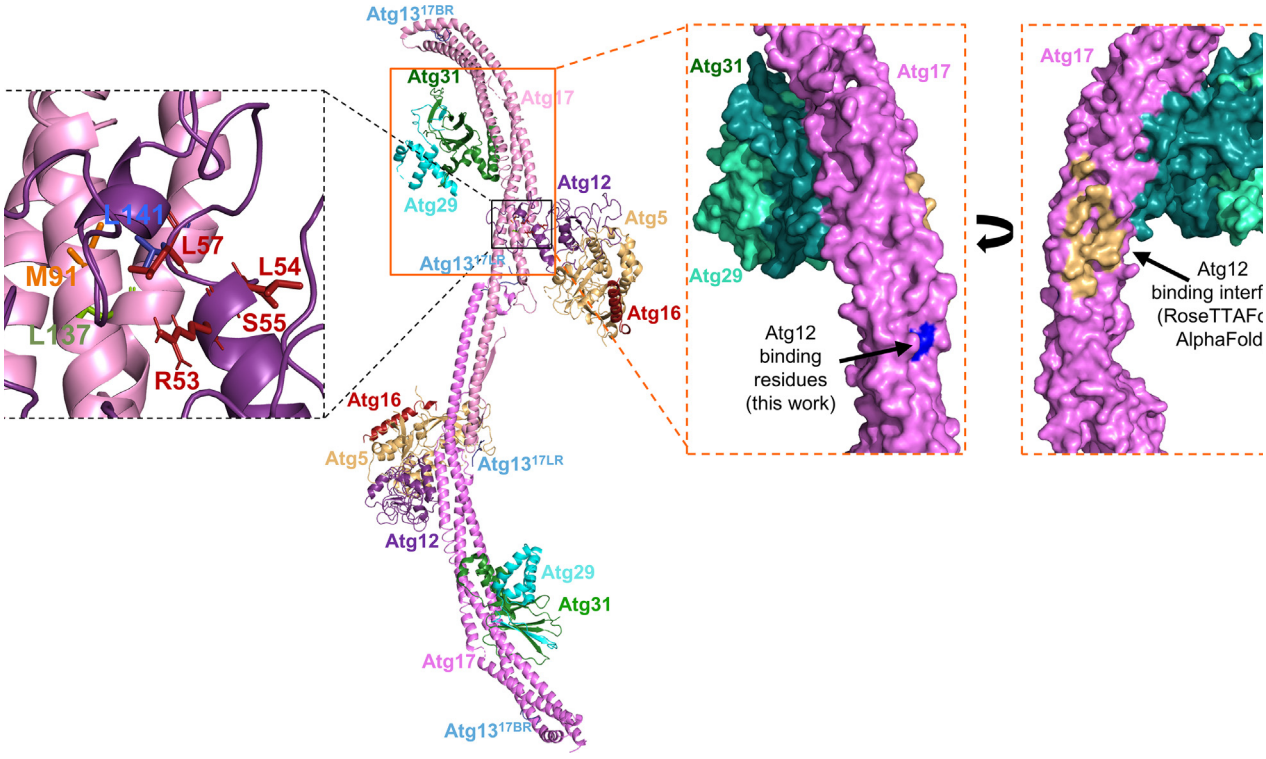

Figure 3. Molecular docking of the Atg17 and E3-like complexes. PDB structures Atg13^{17LR}-Atg13^{17BR}-Atg17-Atg29-Atg31 from *Lachancea thermotolerans* (PDB: 5JHF) and Atg12-Atg5-Atg16N from *Saccharomyces cerevisiae* (PDB: 3W1S) were used. Since the N-terminal region of Atg12 is missing in PDB 3W1S, structure of full length Atg12 was first modeled with the Robetta server (https://robetta.bakerlab.org) and then docked to the Atg17 complex (PDB: 5JHF) using HADDOCK v2.2 (https://www.bonvinlab.org/software/haddock2.2/) and ambiguous interaction constraints derived from our mutagenesis data. The resulting docking model was then combined with the Atg12-Atg5-Atg16N PDB structure by 3D alignment of Atg12 structures using PyMOL software (The PyMOL Molecular Graphics System, Version 2.4.0 Schrödinger, LLC). Left: Detailed view of the residues in Atg12 (red sticks) and Atg17 (green, yellow and blue sticks) identified by reverse two-hybrid selection. Right: Enlarged view of a space-filling model of Atg17, Atg29 and Atg31 showing the Atg12 binding residues identified by reverse two-hybrid selection on one side (highlighted in blue) and the Atg12 binding interface predicted by RoseTTAFold/AlphaFold on the opposite side (highlighted in yellow). The structure of Atg12 is omitted for clarity.

just as does Atg31, which interacts with the concave side of the Atg17 crescent (Figure 3, middle). In addition, we note that the Atg12 binding site in Atg17 is distinct from that reported in the context of a large-scale analysis of eukaryotic protein complexes using RoseTTAFold and AlphaFold[22] (Figure 3 right and Figure S1).

Analysis of the mechanisms involved in recruitment of the E3-like Atg12-Atg5-Atg16 complex to the PAS

As mentioned above, the recruitment of the Atg12-Atg5-Atg16 complex to the PAS is mediated by binding of Atg12 to Atg17, and by the interaction of Atg16 with the PtdIns3P-binding protein, Atg21.[19] To analyze the contribution of these two mechanisms to the autophagy process, we studied the effect of inactivating the Atg12 binding site in Atg17 in the presence or absence of Atg21. ALP assays showed that the inactivation of the binding site of Atg12 in Atg17 has the same inhibitory effect on autophagy as the deletion of *ATG21* (Figure 4A). Additionally, and in agreement with previous work,[19] we found that simultaneous inactivation of the two recruitment mechanisms leads to an even greater reduction in autophagy flux (Figure 4A). However, in contrast to previously reported results, autophagy is not completely blocked in this strain (compare the last two columns), suggesting that alternative mechanisms of recruitment of the Atg12-Atg5-Atg16 complex to the PAS remain. To ensure that this result is not due to residual binding of the Atg17(M91V) mutant to Atg12, we repeated this experiment with a triple mutant (3 M) containing the three mutations identified in the reverse two-hybrid screen, M91V, L137S and L141P. We observed that the triple mutant gives the same result as the M91V mutant (Figure 4A).

To confirm these results, we repeated the experiment by inactivating the Atg17 binding site in Atg12. We found that the deletion of *ATG21*,

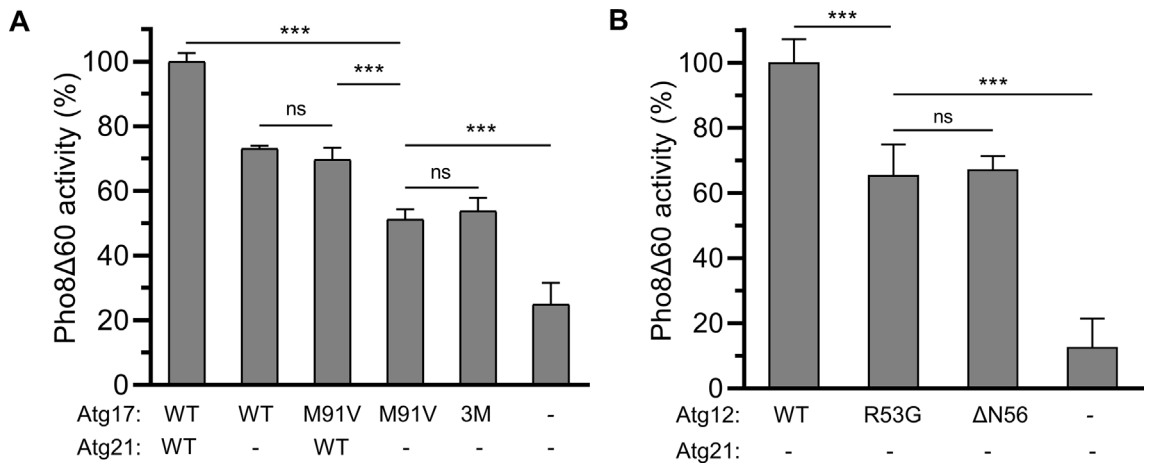

Figure 4. Inhibition of both Atg17- and Atg21-mediated recruitment of the Atg12-Atg5-Atg16 complex significantly impairs but does not ablate autophagy. (**A**) PHO8Δ60 assay. OVY422 (*PHO8Δ60 atg17Δ atg21Δ*) was cotransformed with pAtg21-3FLAG (WT) or vector control pRS315 (−) and p3FLAG-Atg17 (WT), the mutant derivatives M91V and M91V-L137S-L141P (3 M), or vector control pRS313 (−). (**B**) PHO8Δ60 assay. OVY478 (*PHO8Δ60 atg12Δ atg21Δ*) was transformed with p3HA-Atg12 (WT), the mutant derivatives R53G and ΔN56 lacking the N-terminal 56 residues, or vector control pRS315 (−). Cells grown to mid-log phase were starved 4 h in SD-N medium. The PHO8Δ60 assay was carried out as described in Material and Methods and the ALP activity was normalized to the activity of WT (A) or *atg21Δ* (B) cells, which were set to 100%. The mean values are shown with standard deviation ($n = 3$). ***$p > 0.001$, ns: non-significant (One-way Anova).

along with the R53G mutation in Atg12 or with the N-terminal truncation of 56 amino acids (ΔN56), also results in a partial reduction of autophagy, supporting the existence of alternative mechanisms of recruitment of the Atg12-Atg5-Atg16 complex to the PAS (Figure 4B).

PKA-mediated phosphorylation of Atg12 prevents Atg17 binding

Previous work showed that Atg12 is phosphorylated *in vivo*.[17] Additionally, we identified a PKA consensus phosphorylation site (K/R-K/R-X-S/T) conserved in Atg12 orthologs within the *Saccharomyces* clade, which overlaps with the Atg17 binding site identified in this work (Figure 2C). In line with previous studies,[17] Atg12 migrates as a ladder of bands on Western blots and treatment with lambda phosphatase results in a shift to faster migrating species (Figure 5A). The phosphorylated form of Atg12 is also reduced in a strain lacking the three catalytic subunits of PKA (tpk1-3), supporting the idea that Atg12 phosphorylation is due, at least in part, to this protein kinase (Figure 5B). We then used an antibody that specifically recognizes phosphorylated PKA sites (α-p-PKA). Western blot analysis of GFP-Atg12 immunoprecipitates with this antibody confirmed the phosphorylation of this protein by PKA (Figure 5C). Furthermore, the S55A substitution in the PKA consensus site prevents Atg12 phosphorylation, demonstrating that Ser55 is the only residue of Atg12 phosphorylated *in vivo* by PKA (Figure 5C). The previous identification of Ser55 as one of the residues involved in Atg17 binding raises the possibility that PKA regulates the association between Atg12 and Atg17. To test this hypothesis, we pre-incubated purified, bacterially expressed GST-Atg12 with PKA and ATP, and analyzed its interaction with Flag-Atg17 from yeast extracts in GST pull-down assays. Western blot analysis shows that GST-Atg12 is phosphorylated *in vitro* under these conditions (Figure 5D, lower panel) and that this phosphorylation almost completely prevents the interaction with Flag-Atg17 (Figure 5D, upper panel). Furthermore, this effect is due solely to the phosphorylation of the Ser55 residue in Atg12, as binding of the nonphosphorylatable form GST-Atg12(S55A) is unaffected by PKA treatment (Figure 5D, upper panel). Taken together, these results show that PKA phosphorylation of the Ser55 residue in Atg12 prevents its interaction with Atg17.

Interestingly, previous work has shown that PKA-mediated phosphorylation of Atg13 also prevents its interaction with Atg17 and inhibits its association with the PAS.[23] Accordingly, a mutant form of Atg13 that cannot be phosphorylated by PKA is constitutively localized to the PAS.[23] To investigate whether PKA-mediated phosphorylation of Atg12 also inhibits its association with the PAS, we analyzed the localization of Atg5, which is conjugated to Atg12, in strains expressing wild-type Atg12 or the nonphosphorylatable version Atg12(S55A). However, although we confirmed that Atg5 localizes to the PAS upon rapamycin-induced activation of autophagy, we found that the S55A substitution in Atg12 does not result in constitutive localization of Atg5 to the PAS (Figure S2). This could be due to

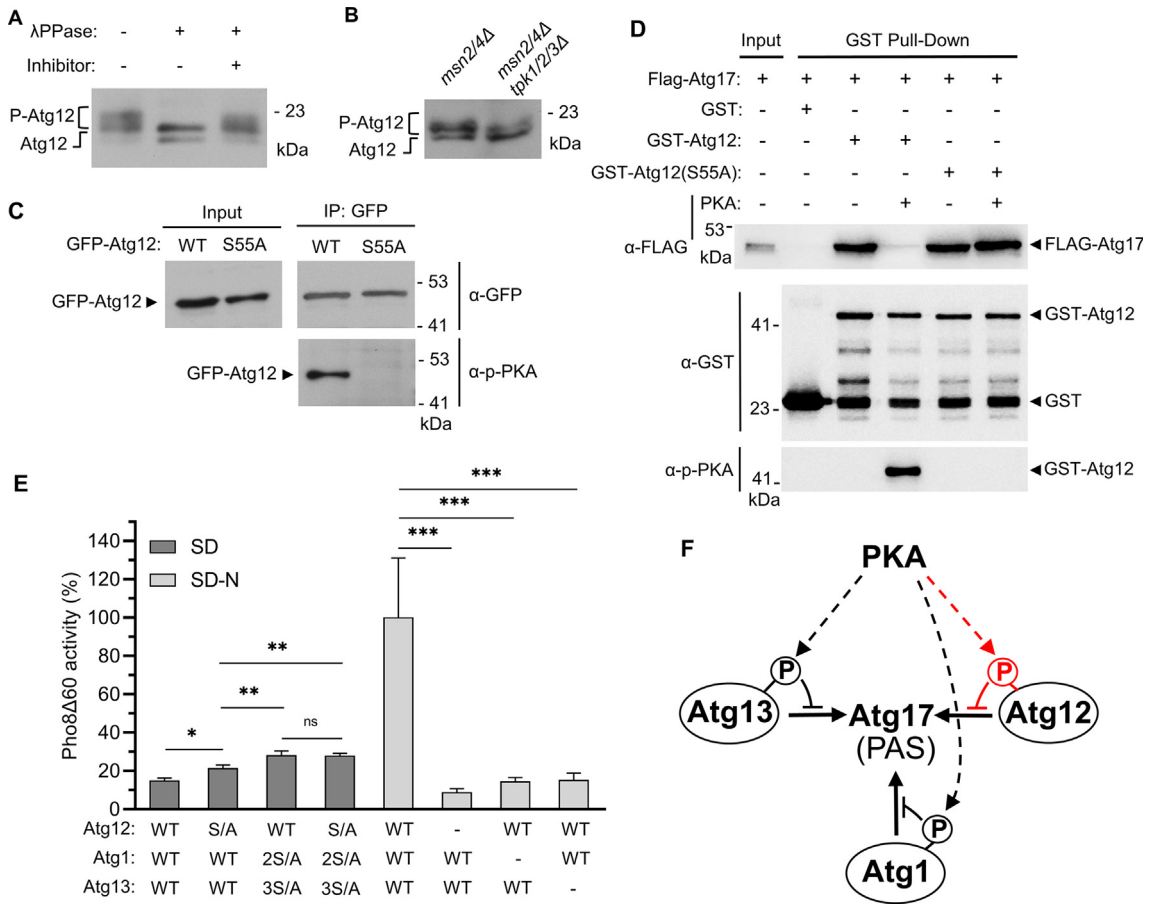

Figure 5. PKA-mediated phosphorylation of Atg12 prevents Atg17 binding. (**A**) HA-Atg12 immunoprecipitates were treated with λ phosphatase (λPPase) with or without phosphatase inhibitor and immunoblotted with anti-HA antibody. Position of the phosphorylated (P) form of Atg12 is indicated. (**B**) OVY465 (*msn2/4Δ*) and OVY464 (*msn2/4Δ tpk1/2/3Δ*) were transformed with p3HA-Atg12 and protein extracts were immunoblotted with anti-HA antibody. (**C**) Immunoprecipitated GFP-Atg12 and S55A mutant derivative were immunoblotted with anti-GFP or anti-P-PKA substrate antibody. (**D**) Pulldown assay of Flag-Atg17 with GST, GST-Atg12 or GST-Atg12(S55A), either pretreated or not with PKA and ATP. Input represents 2% of protein extract used for binding experiment. (**E**) OVY640 was cotransformed with p3HA-Atg12, pAtg1-3HA and pAtg13-3FLAG, or the mutant derivatives p3HA-Atg12(S55A) (S/A), pAtg1(S508A-S515A)-3HA (2S/A), pAtg13(S344A-S437A-S581A)-3FLAG (3S/A) or vector controls (−). Cells were grown to mid-log phase in SD medium (dark grey bar) or starved 4 h in SD-N medium (light grey bar). ALP activity was measured and normalized to WT cells in SD-N (100%). The mean values are shown with standard deviation (n = 3). $^{*}p > 0.05$, $^{**}p > 0.01$, $^{***}p > 0.001$ (One way Anova). (**F**) Schematic representation of the PKA-dependent regulation of the autophagic machinery showing that PKA-mediated phosphorylation of Atg1, Atg13 and Atg12 (dashed arrows) prevents their recruitment to Atg17 (PAS) (plain arrows). The new regulatory mechanism described in this work is highlighted in red.

the fact that the recruitment of the Atg12-Atg5-Atg16 complex to the PAS, unlike that of Atg13, depends not only on its association with Atg17 but also on its interaction with the PtdIns3P-binding protein Atg21,[19] and that the formation of PtdIns3P in turn depends on the Atg1 protein kinase, which like Atg13 is under the control of PKA.[24]

Based on these results, we used an alternative approach to assess the role of PKA in this process. We tested whether simultaneous blockade of the different known regulatory layers by which PKA negatively controls autophagy leads to a constitutive activation of this process, as observed when PKA activity is inhibited.[23] To this end, we transformed a Δ*atg1* Δ*atg13* Δ*atg12* triple mutant strain with plasmids expressing near-endogenous levels of wild-type or mutant forms of Atg1, Atg13 and Atg12 that cannot be phosphorylated by PKA.[23,24] We first verified that cotransformation of the triple mutant strain with the 3 plasmids expressing the wild-type forms of Atg1, Atg13 and Atg12 is required to activate autophagy after a shift to nitrogen-free medium (SD-N) (Figure 5E). As expected, this activation is not detected in nutrient-rich medium (SD) (Figure 5E, first column). Under these growth conditions, expression

of the nonphosphorylatable form Atg12(S55A) (S/A) results in a slight, yet significant, increase in ALP activity (Figure 5E). The increase is even greater when the nonphosphorylatable form Atg1 (S508A-S515A) (2S/A) and Atg13(S344A-S437A-S581A) (3S/A)[23,24] are coexpressed (Figure 5E). However, simultaneous expression of the three mutant forms does not result in a further increase in autophagic flux, which remains much lower than that observed with the wild-type proteins after a shift to a nitrogen-free medium (SD-N) (Figure 5E). Taken together, these results demonstrate that the elimination of the PKA-mediated regulation of Atg12, Atg1 and Atg13 is not sufficient to substantially increase the autophagic flux in nutrient-rich conditions, supporting the existence of additional regulatory layers by which PKA controls the autophagy process.

Discussion

In this study, we investigated the molecular basis of the interaction between the Atg17 scaffold of the Atg1 complex and the Atg12 subunit of the E3-like complex. First, we used the reverse double two-hybrid system (RD2H) to identify mutations in residues critical for protein–protein interaction in both Atg17 and Atg12. We then validated the reverse two-hybrid screen by GST pulldown assays and analyzed the effect of the corresponding mutants on autophagic flux. Furthermore, considering that Atg17 is a scaffold protein with multiple interactors and that the corresponding binding sites are in close proximity to each other, we ensured that the mutations identified in Atg17 specifically prevent Atg12 binding and do not impair its interaction with other proteins of the Atg17 complex such as Atg13 and Atg31, nor the dimerization of Atg17. Notably, all identified residues are in close proximity to each other in the 3D structures of both Atg17 and Atg12, supporting the idea that they belong to the Atg17-Atg12 binding interface. In addition, all the mutations lead to a partial reduction in autophagic flux, which is further decreased when combined with the Δ*atg21* deletion.

The key binding residues in Atg12 and Atg17 were used to generate a docking model of Atg12-Atg5-Atg16 with the Atg17 subcomplex. According to this model, the binding residues in Atg12 are part of an α-helix that appears to form a four-helix bundle with the three helices of Atg17, similar to that described for the binding of Atg31 to Atg17[2] and Figure 3). In the course of this study, a large-scale analysis using RoseTTAFold and AlphaFold addressed the modeling of multiple eukaryotic protein complexes, including that formed by Atg12 and Atg17.[22] The resulting model is consistent with our results for Atg12 but not for Atg17. According to the RoseTTAFold/AlphaFold model, the binding interface in Atg17 is located on the opposite side of the Atg17 crescent, close to the Atg31 binding site and far from the Atg12 binding residues identified in our study (Figure 3, right). This discrepancy demonstrates that experimental data such as those described in our work are necessary to validate models generated using artificial intelligence programs. Furthermore, it was recently reported that the α-helix of Atg12 that mediates Atg17 binding is also involved in the interaction of Atg12 with Atg7 and Atg10 during the ubiquitin-like conjugation cascade,[25] suggesting that Atg17-Atg12 interaction may play a regulatory role in the conjugation of Atg12 to Atg5.

As mentioned above, a previous study showed that Atg17-Atg12 and Atg21-Atg16 binding cooperate to mediate the recruitment of the Atg12-Atg5-Atg16 complex to the PAS.[19] In agreement with this model, the combination of a N-terminal truncation of Atg12 with the Δ*atg21* deletion was reported to completely block autophagy.[19] Here, we analyzed the effect of point mutations in Atg17 and Atg12 that prevent Atg17-Atg12 binding to obtain a more precise analysis of this process. In agreement with previous work, these mutations lead to a reduction in autophagic flux, which is further decreased when combined with the Δ*atg21* deletion. However, in contrast to previously reported results, residual autophagy is still detected in the double mutant. This discrepancy could be due to the use of point mutants instead of a N-terminal truncation of Atg12, although our results suggest that both mutants exhibit the same autophagy defect. The residual autophagy detected in the double mutant support the idea that additional mechanisms can mediate the recruitment of the Atg12-Atg5-Atg16 to the autophagosomal membrane. These mechanisms could involve Atg5 and/or Atg16 since both proteins exhibit membrane-binding capacity.[26,27]

A key finding of our work is the identification of a new regulatory layer by which PKA controls the autophagic machinery. Previous studies showed that PKA, like Tor, plays a key role in regulating autophagy in yeast, and that inhibition of PKA activity, like rapamycin-mediated inhibition of Tor activity, strongly induces autophagy.[23] These studies showed that PKA and Tor independently regulate the Atg1 kinase complex and that PKA phosphorylation of Atg1 and Atg13 inhibits their recruitment to the PAS[23,24] and Figure 5F). Here, we identified an additional regulatory layer that involves the PKA phosphorylation of the Atg12 subunit of the E3-like complex (Figure 5F). We further showed that PKA phosphorylation of Atg12, like that of Atg13, prevents its association with Atg17. However, unlike what has been reported for Atg13, alanine substitution of the phosphorylated residue in Atg12 does not result in a constitutive localization of the Atg12-Atg5 conjugate to the PAS, which could be explained by the fact that recruitment of the E3-like complex is also dependent on the inter-

action of Atg16 with the PtdIns3P-binding protein Atg21.

The PKA phosphorylation sites in Atg13 are Ser344, Ser437 and Ser581.[23] The first two serine residues are relatively close to the Atg17 binding sites in Atg13, 17LR (aa 359–389) and 17BR (aa 424–436),[5] suggesting that phosphorylation of these residues could, as for Atg12, interfere with Atg17 binding. The regulation of Atg1 by PKA is not as well understood since this protein does not directly interact with Atg17, and its recruitment to the PAS should depend on its association with Atg13. The PKA phosphorylation sites in Atg1, Ser508 and Ser515, are outside the Atg13 binding domain,[5,24] and PKA phosphorylation of Atg1 and Atg13 does not alter the interaction between these two proteins,[23] suggesting a different regulatory mechanism. Finally, while inhibition of PKA activity is sufficient to induce autophagy activity,[23] we found that simultaneous elimination of the PKA phosphorylation sites in Atg1, Atg13, and Atg12 only results in a small increase in autophagic flux under nutrient-rich conditions, supporting the idea that there are additional regulatory layers by which PKA controls the autophagic machinery.

Interestingly, the N-terminal region of Atg12 that binds Atg17 is not conserved in mammalian ATG12. However, another subunit of the mammalian E3-like complex, ATG16L1, interacts with the functional counterpart of Atg17, FIP200, and this interaction involves a region of ATG16L1 that is also not conserved in its yeast homolog.[28,29] These differences suggest, as noted previously,[19] that the association between the scaffold protein of the autophagy initiation complex and the lipidation machinery is conserved in yeast and mammals, although it involves different subunits of the E3-like complex. Strikingly, PKA also phosphorylates ATG16L1, driving the phosphorylation-dependent degradation of this protein.[30] The residue phosphorylated by PKA in ATG16L1, Ser268, is located in the region between the coiled-coil and WD domains, which also contains the two FIP200 binding sites (230–250 and 288–300) located on either side of the phosphorylated residue.[28,29,31] Based on these observations, it is tempting to speculate that PKA phosphorylation of ATG16L1, similar to that of Atg12 in yeast, may regulate the association of the E3-like complex with the scaffold protein of the autophagy initiation complex.

Material and Methods

Strains and genetic methods

The *S. cerevisiae* strains used in this study are described in Table S1. PCR-based gene deletion with the kanMX4, natMX4 and hphNT1 markers, were performed as described previously.[32,33] Strains expressing *PHO8Δ60* from the *GPD1* promoter were generated by a PCR-based gene modification method using pYM-N15[34] or pYM-N15(U), a pYM-N15 derivative in which the pAgTEF-nat sequence has been replaced by the *URA3* coding sequence with a 155-bp 5′ sequence. Standard genetic methods were followed, and yeast cultures were grown in YPAD (yeast extract-peptone-adenine-dextrose) or SD (synthetic dextrose) medium lacking appropriate supplements when plasmid selection was required.[35] Yeast cells were grown to mid-log phase and when indicated, autophagy was induced by nitrogen starvation in SD-N medium for 4 h (0.17% yeast nitrogen base without amino acids and 2% glucose).

Plasmids

Plasmids used in this study are listed in Table S2 and were constructed for the current study except pGBKT7-Atg16, pAtg21-3FLAG and pGBKT7-Atg5,[16] pLexA-TSG101[20] and pRS316-GFP-AUT7.[36] Two-hybrid plasmids encoding Gal4 Binding Domain (GBD) or Gal4 Activation Domain (GAD) fusions to Atg12, Atg13, Atg16, Atg17 and Atg31 were constructed by cloning the corresponding coding sequence in the polylinker of pGBKT7, pACT2 or pGAD424 (Clontech). Reverse two-hybrid plasmids pACT2-Atg17-PTAP and pACT2-Atg12-PTAP were obtained by cloning the Atg17 and Atg12 (aa 1–185) coding sequences in the polylinker of pACT2-PTAP.[20] pGBKT7-Atg17-PTAP was generated by cloning the Atg17-PTAP sequence from pACT2-Atg17-PTAP in the polylinker of pGBKT7. pGEX6P1-Atg12 was constructed by cloning the Atg12 coding sequence in the polylinker of pGEX6P1 (GE Healthcare). p3FLAG-Atg17, p3HA-Atg12 and pGFP-Atg12 expressing near endogenous levels of N-terminally triple FLAG-tagged Atg17 and triple HA- or GFP-tagged Atg12 under the control of their native promoter and terminator are derivative of centromeric plasmids pRS313 and pRS315[37] containing the Atg17 or Atg12 coding sequences with ∼500 bp 5′ sequence and ∼250 bp 3′ sequence. pAtg1-3HA and pAtg13-3FLAG expressing near-endogenous levels of C-terminally triple HA-tagged Atg1 and triple FLAG-tagged Atg13 under the control of their native promoter and the *ADH1* terminator are derivatives of centromeric plasmids pRS314 and pRS313[37] containing the Atg1 and Atg13 coding sequence with ∼500 bp or ∼1000 bp 5′ sequence, respectively. Missense or truncating mutations in Atg1, Atg12, Atg13 and Atg17 were obtained by random PCR mutagenesis (reverse two-hybrid screens) or site-directed mutagenesis.

Yeast two-hybrid and β-galactosidase assays

S. cerevisiae strains CTY10-5d and Y187 were used for transformation of LexA fusion proteins and GBD fusion proteins, respectively (Table S1). Two-hybrid interactions were determined by X-gal filter assays as described previously[38] and devel-

oped for 2–4 h. Eight independent transformants were tested and two representatives are shown.

Reverse two-hybrid screening

Reverse two hybrid screens to identify mutations in Atg12 and Atg17 that disrupt Atg17-Atg12 binding were carried out as described previously.[20] Briefly, random mutagenesis of the Atg12 and Atg17 sequences was performed using pACT2-Atg12-PTAP and pACT2-Atg17-PTAP as template and Taq polymerase with 30 rounds of PCR (94 °C for 30 s, 55 °C for 30 s, and 72 °C for 1 min). The primers used for mutagenic PCR were OV621 5′-CAC TGT CAC CTG GTT GGA CGG-3′ and OV622 5′-CTA TAG ATC AGA GGT TAC ATGGC-3′, which amplify a PCR product containing the Atg12-PTAP and Atg17-PTAP fusion flanked by 5′ and 3′ sequences identical to the pACT2 vector digested with Nco1 and Xho1. Strain OVY216 was first transformed with the pGBKT7-Atg17 or pGBKT7-Atg12 bait constructs and the resulting transformants were co-transformed with the linearized vector pACT2 and the PCR mutagenic product containing the Atg12-PTAP or Atg17-PTAP sequences, respectively, to allow gap-repair cloning of pACT2-based plasmids expressing randomly mutated Atg12-PTAP or Atg17-PTAP. Transformants were simultaneously selected for Ura- and His+ phenotypes as previously described[20] and mutated plasmids were recovered from 14 (Atg12 screen) and 15 (Atg17 screen) large colonies. The isolated plasmids were cotransformed with pGBKT7-Atg17 (Atg12 screen) and pGBKT7-Atg12 (Atg17 screen) in strain Y187, or with pLexA-TSG101 in strain CTY10-5d, to confirm that mutations in Atg12-PTAP or Atg17-PTAP disrupt Atg17-Atg12 binding but do not truncate the protein and thus do not impair PTAP-mediated interaction with LexA-TSG101. All Atg17 mutants and four Atg12 mutants behaved as expected. Finally, loss of binding mutations in Atg12 and Atg17 were identified by DNA sequencing. Six of the Atg17 mutants containing several mutations were not further characterized.

Immunoblot analysis

Yeast protein extracts were prepared by the NaOH/TCA lysis method[39] and analyzed by SDS/PAGE and immunoblotting with anti-GFP (G-1544; Sigma-Aldrich), anti-Flag (M2; Sigma-Aldrich), anti-HA (16B12; BioLegend), anti-actin (C4; MP Biomedicals), and anti-Phospho-PKA substrate (100G7E, Cell Signaling Technology) antibodies. Immunoblots were developed with ECLPlus reagent (Pierce).

For immunoprecipitation and λ phosphatase treatment of HA-Atg12, OVY472 (*atg12Δ*) was transformed with p3HA-Atg12 and protein extracts were prepared by cell disruption with glass beads in IP buffer (50 mM Hepes, pH 7.5/150 mM NaCl/0.1% Triton X-100/1 mM DTT/10% glycerol/2.5 mM NaF/Complete protease inhibitor mixture (Roche)). Protein lysates (400 μg) were incubated with 20 μl of anti-HA (Roche) affinity matrix for 1 h on a rotating wheel and λ phosphatase treatment of HA-Atg12 immunoprecipitates was carried out for 30 min at 37 °C in 100 μl reaction mixtures containing 2 mM $MnCl_2$ and 400 mU of λ phosphatase (Biolabs). Where indicated, 10 mM Na_3VO_4 was used as phosphatase inhibitor. Immunoprecipitated extracts were analyzed by SDS/PAGE and immunoblotting with monoclonal anti-HA (16B12; BioLegend) antibodies. Antibodies were detected by enhanced chemiluminescence with ECLPlus reagents (Pierce).

For immunoprecipitation of GFP-Atg12, OVY472 (*atg12Δ*) was transformed with pGFP-Atg12 or mutant derivatives, and protein extracts were prepared by cell disruption with glass beads in RIPA buffer (10 mM Tris-HCl, pH 7.5/150 mM NaCl/0.5 mM EDTA/0.1% SDS/1% Triton X-100/1% sodium deoxycholate/Complete protease inhibitor mixture (Roche)/1 mM DTT/2.5 mM NaF). Following centrifugation, the supernatant was diluted three-fold with the same buffer but without detergent and incubated with 10 μl of GFP-Trap Agarose (ChromoTek) and rotated at 4 °C for 2 h. Resin was washed 3 times with the same buffer without detergent and immunoprecipitated extracts were analyzed as described above with anti-GFP (G-1544; Sigma-Aldrich) and anti-Phospho-PKA substrate (100G7E, Cell Signaling Technology) antibodies.

Pulldown assays

OVY379 (*atg17Δ*) was transformed with p3FLAG-Atg17 (WT) or mutant derivatives, and yeast protein extracts were prepared by cell disruption with glass beads in IP buffer plus 1% (vol/vol) Triton X-100. Recombinant GST-Atg12 and mutant derivatives were purified from *Escherichia coli* BL21 (Novagen) as described previously.[40] Sepharose beads loaded with GST or GST fusion proteins were incubated in IP buffer plus 0.35% (vol/vol) Triton X-100 with 500 μg of yeast protein lysates at 4 °C for one hour. After three washes with the same buffer, beads were boiled in sample buffer and proteins were separated by 10% SDS-PAGE and analyzed by immunoblotting with anti-GST (B-14; Santa Cruz) and anti-Flag (M2; Sigma-Aldrich) antibodies.

The PKA treatment of GST fusion proteins was carried out for 40 min at room temperature in 10 μl reaction mixture containing 40 mM Tris-HC,l pH 7.5, 20 mM $MgCl_2$, 0.4 mM ATP and 50u cAMP-dependent protein kinase (Promega). After two washes with STE buffer (10 mM Tris-HCl, pH 8.0/1 mM EDTA/150 mM NaCl), beads loaded with GST fusion proteins were incubated with yeast protein lysates as described above.

PHO8Δ60 assays

ALP activity measurement was performed essentially as previously described.[21] Yeast cells were grown to mid-log phase in SD medium, starved 4 h in SD-N medium, and cells were mechanically lysed with glass beads 10 x 10 s in 400 μl of ALP buffer (100 mM Tris-HCl, pH9, 10 mM $MgCl_2$, 10 μM $ZnSO_4$, 1 mM PMSF) at 4 °C. Protein extracts were cleared by 5 min centrifugation (13,000 g) at 4 °C. Assays were performed in triplicate: 50 μl of supernatant was mixed with 450 μl ALP buffer prewarmed at 30 °C. Reactions were initiated by adding 5 mM p-nitrophenyl phosphate and were incubated for 10 min at 30 °C before stopping the reaction with 500 μl of 2 M glycine, pH 11. The fluorescence emission of the product α-napthol (λ_{ex} = 345 and λ_{em} = 472) was measured using a Synergy HTX Multimode Reader (BioTek) and the protein concentration of the cell extract was determined using the Pierce™ BCA protein assay (Thermo Scientific). ALP activity was then normalized to wild-type controls.

Statistical analyses

Data represent the means of three independent biological replicates ± standard deviation (SD). Statistical analyses were accomplished by using one-way ANOVA. Comparisons with a *p*-value <0.05 were considered statistically significant. Non-significant differences are indicated (ns).

CRediT authorship contribution statement

Miranda Bueno-Arribas: Writing – review & editing, Visualization, Validation, Investigation, Formal analysis, Conceptualization. **Celia Cruz-Cuevas:** Investigation. **Beatriz Monforte-Martinez:** Investigation. **María-Angeles Navas:** Writing – review & editing, Investigation. **Ricardo Escalante:** Writing – review & editing, Resources, Project administration, Funding acquisition. **Olivier Vincent:** Writing – review & editing, Writing – original draft, Supervision, Resources, Project administration, Methodology, Investigation, Funding acquisition, Conceptualization.

DECLARATION OF COMPETING INTEREST

The authors declare that they have no known competing financial interests or personal relationships that could have appeared to influence the work reported in this paper.

Acknowledgments

This work has been supported by grants PGC2018-093604-B-I00 (MCIU/AEI/FEDER, UE) and PID2021-127355OB-I00 (MICIU/AEI/10.13039/501100011033/FEDER,UE). M.B. has been supported by a fellowship from the Spanish "Ministerio de Ciencia, Innovación y Universidades" and C.C. has been supported by the Garantía Juvenil Program from Comunidad de Madrid. We thank Carmen Lisset Flores for yeast strains.

Appendix A. Supplementary material

Supplementary material to this article can be found online at https://doi.org/10.1016/j.jmb.2025.168954.

Received 2 December 2024;
Accepted 11 January 2025;
Available online 16 January 2025

Keywords:
autophagy;
ATG17;
ATG12;
PKA;
reverse two-hybrid

References

1. Noda, N.N., (2024). Structural view on autophagosome formation. *FEBS Lett.* **598**, 84–106. https://doi.org/10.1002/1873-3468.14742.
2. Ragusa, M.J., Stanley, R.E., Hurley, J.H., (2012). Architecture of the Atg17 complex as a scaffold for autophagosome biogenesis. *Cell* **151**, 1501–1512. https://doi.org/10.1016/j.cell.2012.11.028.
3. Fujioka, Y., Suzuki, S.W., Yamamoto, H., Kondo-Kakuta, C., Kimura, Y., Hirano, H., Akada, R., Inagaki, F., Ohsumi, Y., Noda, N.N., (2014). Structural basis of starvation-induced assembly of the autophagy initiation complex. *Nature Struct. Mol. Biol.* **21**, 513–521. https://doi.org/10.1038/nsmb.2822.
4. Rao, Y., Perna, M.G., Hofmann, B., Beier, V., Wollert, T., (2016). The Atg1-kinase complex tethers Atg9-vesicles to initiate autophagy. *Nature Commun.* **7**, 10338. https://doi.org/10.1038/ncomms10338.
5. Yamamoto, H., Fujioka, Y., Suzuki, S.W., Noshiro, D., Suzuki, H., Kondo-Kakuta, C., Kimura, Y., Hirano, H., Ando, T., Noda, N.N., Ohsumi, Y., (2016). The intrinsically disordered protein Atg13 mediates supramolecular assembly of autophagy initiation complexes. *Dev. Cell* **38**, 86–99. https://doi.org/10.1016/j.devcel.2016.06.015.
6. Sawa-Makarska, J., Baumann, V., Coudevylle, N., von Bülow, S., Nogellova, V., Abert, C., Schuschnig, M., Graef, M., Hummer, G., Martens, S., (2020). Reconstitution of autophagosome nucleation defines Atg9 vesicles as seeds for membrane formation. *Science* **369** https://doi.org/10.1126/science.aaz7714.
7. Hu, Z., Raucci, S., Jaquenoud, M., Hatakeyama, R., Stumpe, M., Rohr, R., Reggiori, F., De Virgilio, C., Dengjel, J., (2019). Multilayered control of protein turnover by TORC1 and Atg1. *Cell Rep.* **28**, 3486–3496. e6. https://doi.org/10.1016/j.celrep.2019.08.069.
8. Hitomi, K., Kotani, T., Noda, N.N., Kimura, Y., Nakatogawa, H., (2023). The Atg1 complex, Atg9, and Vac8 recruit PI3K

complex I to the pre-autophagosomal structure. *J. Cell Biol.* **222** https://doi.org/10.1083/jcb.202210017.
9. Vincent, O., Antón-Esteban, L., Bueno-Arribas, M., Tornero-Écija, A., Navas, M.-Á., Escalante, R., (2021). The WIPI gene family and neurodegenerative diseases: insights from yeast and dictyostelium models. *Front. Cell Dev. Biol.* **9**, https://doi.org/10.3389/fcell.2021.737071 737071.
10. Obara, K., Sekito, T., Niimi, K., Ohsumi, Y., (2008). The Atg18-Atg2 complex is recruited to autophagic membranes via phosphatidylinositol 3-phosphate and exerts an essential function. *J. Biol. Chem.* **283**, 23972–23980. https://doi.org/10.1074/jbc.M803180200.
11. Gómez-Sánchez, R., Rose, J., Guimarães, R., Mari, M., Papinski, D., Rieter, E., Geerts, W.J., Hardenberg, R., Kraft, C., Ungermann, C., Reggiori, F., (2018). Atg9 establishes Atg2-dependent contact sites between the endoplasmic reticulum and phagophores. *J. Cell Biol.* **217**, 2743–2763. https://doi.org/10.1083/jcb.201710116.
12. Kotani, T., Kirisako, H., Koizumi, M., Ohsumi, Y., Nakatogawa, H., (2018). The Atg2-Atg18 complex tethers pre-autophagosomal membranes to the endoplasmic reticulum for autophagosome formation. *PNAS* **115**, 10363–10368. https://doi.org/10.1073/pnas.1806727115.
13. Osawa, T., Kotani, T., Kawaoka, T., Hirata, E., Suzuki, K., Nakatogawa, H., Ohsumi, Y., Noda, N.N., (2019). Atg2 mediates direct lipid transfer between membranes for autophagosome formation. *Nature Struct. Mol. Biol.* **26**, 281–288. https://doi.org/10.1038/s41594-019-0203-4.
14. Juris, L., Montino, M., Rube, P., Schlotterhose, P., Thumm, M., Krick, R., (2015). PI3P binding by Atg21 organises Atg8 lipidation. *EMBO J.* **34**, 955–973. https://doi.org/10.15252/embj.201488957.
15. Munzel, L., Neumann, P., Otto, F.B., Krick, R., Metje-Sprink, J., Kroppen, B., Karedla, N., Enderlein, J., Meinecke, M., Ficner, R., Thumm, M., (2021). Atg21 organizes Atg8 lipidation at the contact of the vacuole with the phagophore. *Autophagy* **17**, 1458–1478. https://doi.org/10.1080/15548627.2020.1766332.
16. Bueno-Arribas, M., Cruz-Cuevas, C., Navas, M.-A., Escalante, R., Vincent, O., (2023). Coiled-coil-mediated dimerization of Atg16 is required for binding to the PROPPIN Atg21. *Open Biol.* **13**, https://doi.org/10.1098/rsob.230192 230192.
17. Mizushima, N., Noda, T., Yoshimori, T., Tanaka, Y., Ishii, T., George, M.D., Klionsky, D.J., Ohsumi, M., Ohsumi, Y., (1998). A protein conjugation system essential for autophagy. *Nature* **395**, 395–398. https://doi.org/10.1038/26506.
18. Mizushima, N., Noda, T., Ohsumi, Y., (1999). Apg16p is required for the function of the Apg12p-Apg5p conjugate in the yeast autophagy pathway. *EMBO J.* **18**, 3888–3896. https://doi.org/10.1093/emboj/18.14.3888.
19. Harada, K., Kotani, T., Kirisako, H., Sakoh-Nakatogawa, M., Oikawa, Y., Kimura, Y., Hirano, H., Yamamoto, H., Ohsumi, Y., Nakatogawa, H., (2019). Two distinct mechanisms target the autophagy-related E3 complex to the pre-autophagosomal structure. *Elife 8*. https://doi.org/10.7554/eLife.43088.
20. Vincent, O., Gutierrez-Nogués, A., Trejo-Herrero, A., Navas, M.-A., (2020). A novel reverse two-hybrid method for the identification of missense mutations that disrupt protein-protein binding. *Sci. Rep.* **10**, 21043. https://doi.org/10.1038/s41598-020-77992-1.
21. Araki, Y., Kira, S., Noda, T., (2017). Quantitative assay of macroautophagy using Pho8△60 assay and GFP-cleavage assay in yeast. *Methods Enzymol.* **588**, 307–321. https://doi.org/10.1016/bs.mie.2016.10.027.
22. Humphreys, I.R., Pei, J., Baek, M., Krishnakumar, A., Anishchenko, I., Ovchinnikov, S., Zhang, J., Ness, T.J., Banjade, S., Bagde, S.R., Stancheva, V.G., Li, X.-H., Liu, K., Zheng, Z., Barrero, D.J., Roy, U., Kuper, J., Fernández, I.S., Szakal, B., Branzei, D., Rizo, J., Kisker, C., Greene, E. C., Biggins, S., Keeney, S., Miller, E.A., Fromme, J.C., Hendrickson, T.L., Cong, Q., Baker, D., (2021). Computed structures of core eukaryotic protein complexes. *Science* **374**, https://doi.org/10.1126/science.abm4805 eabm4805.
23. Stephan, J.S., Yeh, Y.-Y., Ramachandran, V., Deminoff, S. J., Herman, P.K., (2009). The Tor and PKA signaling pathways independently target the Atg1/Atg13 protein kinase complex to control autophagy. *PNAS* **106**, 17049–17054. https://doi.org/10.1073/pnas.0903316106.
24. Budovskaya, Y.V., Stephan, J.S., Deminoff, S.J., Herman, P.K., (2005). An evolutionary proteomics approach identifies substrates of the cAMP-dependent protein kinase. *PNAS* **102**, 13933–13938. https://doi.org/10.1073/pnas.0501046102.
25. Popelka, H., Lahiri, V., Hawkins, W.D., da Veiga Leprevost, F., Nesvizhskii, A.I., Klionsky, D.J., (2023). The intrinsically disordered N terminus in Atg12 from yeast is necessary for the functional structure of the protein. *Int. J. Mol. Sci.* **24** https://doi.org/10.3390/ijms242015036.
26. Popelka, H., Reinhart, E.F., Metur, S.P., Leary, K.A., Ragusa, M.J., Klionsky, D.J., (2021). Membrane binding and homodimerization of Atg16 via two distinct protein regions is essential for autophagy in yeast. *J. Mol. Biol.* **433**, https://doi.org/10.1016/j.jmb.2021.166809 166809.
27. Romanov, J., Walczak, M., Ibiricu, I., Schüchner, S., Ogris, E., Kraft, C., Martens, S., (2012). Mechanism and functions of membrane binding by the Atg5-Atg12/Atg16 complex during autophagosome formation. *EMBO J.* **31**, 4304–4317. https://doi.org/10.1038/emboj.2012.278.
28. Gammoh, N., Florey, O., Overholtzer, M., Jiang, X., (2013). Interaction between FIP200 and ATG16L1 distinguishes ULK1 complex-dependent and -independent autophagy. *Nature Struct. Mol. Biol.* **20**, 144–149. https://doi.org/10.1038/nsmb.2475.
29. Nishimura, T., Kaizuka, T., Cadwell, K., Sahani, M.H., Saitoh, T., Akira, S., Virgin, H.W., Mizushima, N., (2013). FIP200 regulates targeting of Atg16L1 to the isolation membrane. *EMBO Rep.* **14**, 284–291. https://doi.org/10.1038/embor.2013.6.
30. Zhao, X., Nedvetsky, P., Stanchi, F., Vion, A.-C., Popp, O., Zühlke, K., Dittmar, G., Klussmann, E., Gerhardt, H., (2019). Endothelial PKA activity regulates angiogenesis by limiting autophagy through phosphorylation of ATG16L1. *Elife* **8** https://doi.org/10.7554/eLife.46380.
31. Fujita, N., Morita, E., Itoh, T., Tanaka, A., Nakaoka, M., Osada, Y., Umemoto, T., Saitoh, T., Nakatogawa, H., Kobayashi, S., Haraguchi, T., Guan, J.-L., Iwai, K., Tokunaga, F., Saito, K., Ishibashi, K., Akira, S., Fukuda, M., Noda, T., Yoshimori, T., (2013). Recruitment of the autophagic machinery to endosomes during infection is mediated by ubiquitin. *J. Cell Biol.* **203**, 115–128. https://doi.org/10.1083/jcb.201304188.
32. Wach, A., Brachat, A., Pöhlmann, R., Philippsen, P., (1994). New heterologous modules for classical or PCR-based gene disruptions in *Saccharomyces cerevisiae.*

Yeast **10**, 1793–1808. https://doi.org/10.1002/yea.320101310.
33. Goldstein, A.L., McCusker, J.H., (1999). Three new dominant drug resistance cassettes for gene disruption in *Saccharomyces cerevisiae. Yeast* **15**, 1541–1553. https://doi.org/10.1002/(SICI)1097-0061(199910)15:14<1541::AIDYEA476>3.0.CO;2-K.
34. Noda, T., Klionsky, D.J., (2008). The quantitative Pho8Delta60 assay of nonspecific autophagy. *Methods Enzymol.* **451**, 33–42. https://doi.org/10.1016/S0076-6879(08)03203-5.
35. Rose, M.D., Winston, F., Hieter, P., (1990). Methods in Yeast Genetics: A Laboratory Course Manual. Cold Spring Harb. Press, NY.
36. Suzuki, K., Kirisako, T., Kamada, Y., Mizushima, N., Noda, T., Ohsumi, Y., (2001). The pre-autophagosomal structure organized by concerted functions of APG genes is essential for autophagosome formation. *EMBO J.* **20**, 5971–5981. https://doi.org/10.1093/emboj/20.21.5971.
37. Sikorski, R., Hieter, P., (1989). A system of shuttle vectors and yeast host strains designed for efficient manipulation of DNA in *Saccharomyces ceratisiae. Genetics* **122**, 19–27. https://doi.org/10.1080/00362178385380431.
38. Yang, X., Hubbard, E.J., Carlson, M., (1992). A protein kinase substrate identified by the two-hybrid system. *Science* **257**, 680–682. https://doi.org/10.1126/science.1496382.
39. Volland, C., Urban-Grimal, D., Géraud, G., Haguenauer-Tsapis, R., (1994). Endocytosis and degradation of the yeast uracil permease under adverse conditions. *J. Biol. Chem.* **269**, 9833–9841. https://doi.org/10.1016/S0021-9258(17)36959-4.
40. Vincent, O., Rainbow, L., Tilburn, J., Arst, H.N.J., Peñalva, M.A., (2003). YPXL/I is a protein interaction motif recognized by aspergillus PalA and its human homologue, AIP1/Alix. *Mol. Cell. Biol.* **23**, 1647–1655. https://doi.org/10.1128/MCB.23.5.1647-1655.2003.